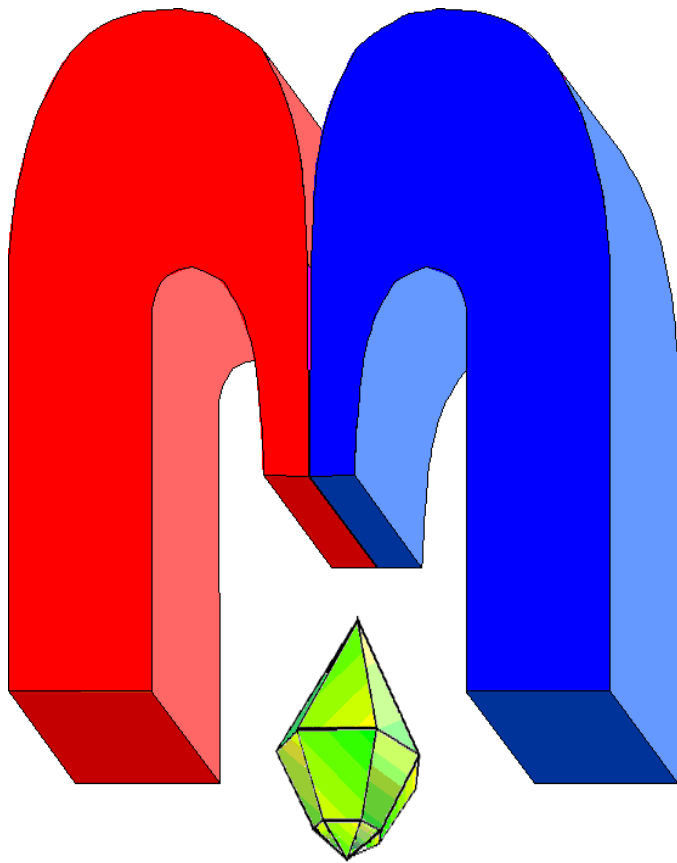


ISSN 2072-5981
doi: 10.26907/mrsej



***Magnetic
Resonance
in Solids***

Electronic Journal

Volume 26

Issue 2

Article No 24216

1-14 pages

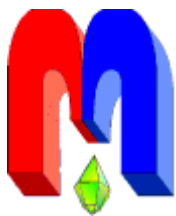
June, 6

2024

doi: 10.26907/mrsej-24216

<http://mrsej.kpfu.ru>

<https://mrsej.elpub.ru>



Established and published by Kazan University*
Endorsed by International Society of Magnetic Resonance (ISMAR)
Registered by Russian Federation Committee on Press (#015140),
August 2, 1996
First Issue appeared on July 25, 1997

© Kazan Federal University (KFU)†

"Magnetic Resonance in Solids. Electronic Journal" (MRSej) is a peer-reviewed, all electronic journal, publishing articles which meet the highest standards of scientific quality in the field of basic research of a magnetic resonance in solids and related phenomena.

Indexed and abstracted by
Web of Science (ESCI, Clarivate Analytics, from 2015), Scopus (Elsevier, from 2012), RusIndexSC (eLibrary, from 2006), Google Scholar, DOAJ, ROAD, CyberLeninka (from 2006), SCImago Journal & Country Rank, etc.

Editor-in-Chief

Boris **Kochelaev** (KFU, Kazan)

Honorary Editors

Jean **Jeener** (Universite Libre de Bruxelles, Brussels)

Raymond **Orbach** (University of California, Riverside)

Executive Editor

Yurii **Proshin** (KFU, Kazan)

mrsej@kpfu.ru



This work is licensed under a [Creative Commons Attribution-ShareAlike 4.0 International License](https://creativecommons.org/licenses/by-sa/4.0/).

 This is an open access journal which means that all content is freely available without charge to the user or his/her institution. This is in accordance with the [BOAI definition of open access](https://www.boai.ru/).

Technical Editors

Maxim **Avdeev** (KFU, Kazan)
Vadim **Tumanov** (KFU, Kazan)
Fail **Sirae**v (KFU, Kazan)

Editors

Vadim **Atsarkin** (Institute of Radio Engineering and Electronics, Moscow)

Yurij **Bunkov** (CNRS, Grenoble)

Mikhail **Eremin** (KFU, Kazan)

David **Fushman** (University of Maryland, College Park)

Hugo **Keller** (University of Zürich, Zürich)

Yoshio **Kitaoka** (Osaka University, Osaka)

Boris **Malkin** (KFU, Kazan)

Alexander **Shengelaya** (Tbilisi State University, Tbilisi)

Jörg **Sichelschmidt** (Max Planck Institute for Chemical Physics of Solids, Dresden)

Haruhiko **Suzuki** (Kanazawa University, Kanazawa)

Murat **Tagirov** (KFU, Kazan)

Dmitrii **Tayurskii** (KFU, Kazan)

Valentine **Zhikharev** (KNRTU, Kazan)

Invited Editor of Special Issue[‡]: Eduard Baibekov (KFU, Kazan)

* Address: "Magnetic Resonance in Solids. Electronic Journal", Kazan Federal University; Kremlevskaya str., 18; Kazan 420008, Russia

† In Kazan University the Electron Paramagnetic Resonance (EPR) was discovered by Zavoisky E.K. in 1944.

‡ Dedicated to Professor Boris Z. Malkin on the occasion of his 85th birthday

Quantum cellular automata based on mixed-valence molecules: Some theoretical hints for cell design

B. Tsukerblat^{1,*}, V. Belonovich^{2,3}, A. Palii²

¹Ben-Gurion University of the Negev, 84105 Beer-Sheva, Israel

²Federal Research Center of Problems of Chemical Physics and Medicine Chemistry,
Chernogolovka 142432, Russia

³Moscow Institute of Physics and Technology, Dolgoprudny 141701, Russia

*E-mail: *tsuker@bgu.ac.il*

(Received May 14, 2024; accepted May 30, 2024; published June 6, 2024)

The purpose of this short review article is to discuss at a simple qualitative level some key requirements the mixed-valence (MV) molecules should meet to be potentially applicable as cells of quantum cellular automata (QCA), and also how different interactions affect their fulfillment. We focus on two requirements, which are closely related to encoding and propagating of binary information within the electronic circuits and power dissipation caused by the logical operations. The physical features behind these requirements are the following: the ability of MV molecules to be efficiently switched between two logical binary states which assumes high polarizability manifesting itself in a strong non-linear cell-cell response and a low heat release caused by molecular rearrangements accompanying logical operations. We discuss the role of such electronic interactions as intramolecular electron transfer, intramolecular interelectronic Coulomb repulsion and the interaction of the excess electrons of a molecular cell with the electric field produced by the neighboring polarized cell. The pivotal role of the interaction of the excess electrons with the molecular vibrations (pseudo Jahn-Teller vibronic coupling) is discussed as well. Finally, the optimal conditions expressed as a parametric regime ensuring simultaneous fulfillment of the aforementioned requirements are discussed.

PACS: 71.70.Ej, 31.00.00, 36.00.00, 36.40.-c, 82.00.00, 85.65.+h

Keywords: quantum cellular automata, cell-cell response, mixed-valency, electron transfer, molecular bistability, Coulomb interaction, pseudo Jahn-Teller effect, power dissipation.

*Dedicated to Professor Boris Z. Malkin,
outstanding scientist who made a significant contribution
to magnetic radiospectroscopy and
dear friend on the occasion of his 85th anniversary*

1. Introduction

Application of the ideas of quantum cellular automata (QCA) to nanoelectronics and computing pioneered by Lent et al [1–10] created a new field of science and nanotechnology with promising applications and advances in physics of nanoobjects. According to new ideas, four quantum dot square capturing two electrons can form a cell, which is able to store binary information encoded in the two charge configurations. The cells interacting through the Coulomb forces can be assembled for the design of various logic elements such as wires, fun-outs, majority logical gates and complex circuits [4–10]. The two charge configurations of square cell in which the interelectronic Coulomb repulsion forces electrons to occupy the diagonals of the square are shown in Fig. 1 along with the indication of the corresponding binary states **0** and **1** (Boolean states). The QCA devices composed of quantum dots have several important potential advantages over the standard Complementary Metal Oxide Semiconductor (CMOS) technology: QCA circuits eliminate the need for current switches because the binary information is encoded in charge

distributions, the power dissipation and heating is strongly reduced, computational pipeline can be achieved by the very nature of the QCA circuits, and finally, the size of the cells is rather small ensuring high density of the devices.

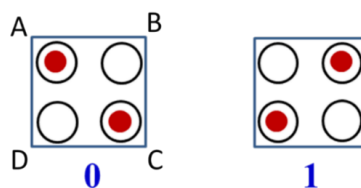


Figure 1. Scheme of a square-planar cell encoding binary information (**0** and **1**) in the two diagonal positions of the electronic pair denoted by red balls. The labels of the dots (redox sites) are used through the article.

More recent idea to scale down the cells by using mixed-valence (MV) molecules with the same topology, suitable properties and electronic structures [4,11–20] promises new advantages, which make them leading candidates to be implemented as QCA cells: unlike quantum dots the molecular systems have a specified chemical composition and identical physical characteristics; by a proper chemical synthesis the molecular clusters can be engineered to have desired physical characteristics that can be controlled by chemical means; molecules can be attached to different types of platforms as monolayers on surfaces. A series of organic and inorganic MV molecular squares suitable for the design of QCA cells have been obtained [16–18]. Advances in supramolecular coordination chemistry have allowed to access to transition-metal compounds of a grid-type architecture comprising two-dimensional arrays of metal ions connecting a set of organic ligands to generate a multiple wiring network [21] that can have direct nanotechnological applications as controlled 2D monolayers of cells.

A large amount of synthetic work aimed at creating prototypes of molecular MV cells has been mainly focused on the design of suitable square-planar structures imitating molecular cells. At the same time, the necessary structural requirements are not sufficient to achieve this ambitious goal since they do not include the physical properties of molecules necessary to ensure their proper functioning in devices. Further progress in the field of QCA has led to a series of works devoted to the study of the functional characteristics of potentially relevant MV molecules in terms of their electronic and vibronic structures. The main interactions employed in the models of molecular MV cells, as well as the theoretical approaches and the routes for possible control of the main functional characteristics of cells are described in detail in [22–35] (see also references therein). We refer also to the recent exhaustive review article reflecting contemporary state-of-art [36].

In this brief review, we discuss electronic and vibronic interactions, which determine the properties of MV molecules, with special emphasis on those properties playing a role in applications in QCA devices. In terms of the mentioned interactions, we will discuss in a qualitative way some necessary key requirements to the properties of MV molecules underlying their application as cells in QCA gates and circuits. These requirements, which will be discussed in more detail are the ability of efficient switching between two charge configurations encoding binary information and the low heat release accompanying switching events in MV cells.

2. Electronic interactions playing a key role in the QCA concept

In the four-dot molecular QCA cell represented by the square-planar (tetrameric) MV molecule the two excess electrons can be distributed in six different ways among the four redox sites.

Two of these distributions, or alternatively, electronic configurations, are energetically preferable because they correspond to the minimum of the interelectronic Coulomb energy. These are the electronic configurations in which the two electrons occupy the pairs of sites situated along diagonals AC or BD of the square. As mentioned just these two diagonal-type configurations (d -configurations) can be associated with the Boolean states $\mathbf{0}$ and $\mathbf{1}$, which makes them suitable to encode binary information. The remaining four electronic distributions in which the electrons are localized along the sides of the square, or alternatively, neighboring configurations (n -configurations), form the excited Coulomb states which are usually much higher in energy because the Coulomb energy gap U between d and n configurations typically exceeds all other intra- and intermolecular interactions. This situation is schematically shown in Fig. 2a.

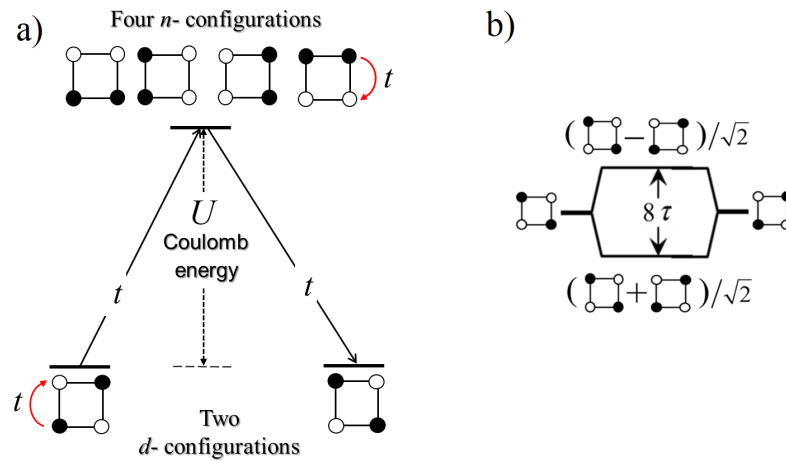


Figure 2. Schematic images of two d - and four n -configurations separated by the intracell Coulomb energy gap U and one-electron transfer processes (red arrows), which transform one of the d -configurations (left) into one of the n -configurations and then the excited n -configuration into the second d -configurations (right) (a), as well as splitting of the ground Coulomb manifold by the effective second-order electron transfer in the strong Coulomb interaction limit (b).

The energy gap U describing the intracell Coulomb interaction is the first key parameter responsible for the properties of the cell. The second key interaction is the one-electron transfer, which transforms different electronic configurations to each other. Typically, only the transfer processes occurring between the nearest neighboring sites (i. e. along the edges of the square) produce notable contributions, while the diagonal-type transfer can be neglected. The electron transfer is depicted by the red arrows in Fig. 2a. This interaction is described by the transfer parameter t , which represents the matrix element of the electronic Hamiltonian linking the two electronic configurations differing from each other in the position of one excess electron. As far as only the transfer processes along the edges are operative, each transfer event changes the interelectronic distance transforming thus one of d -configuration to one of n -configuration. This is shown by black arrows in Fig. 2a. This means that the intracell Coulomb interaction creates the barrier impeding the electron transfer. The most important for QCA is the case when the height of the Coulomb barrier considerably exceeds the energy of the electron transfer, that is the inequality $U \gg t$ holds. In this case termed “limit of strong Coulomb interaction” the electron transfer is strongly reduced and acts as a second-order contribution with the effective second-order transfer parameter $\tau = t^2/U$, which can be regarded as one particular contribution to the second-order two-electron transfer matrix elements linking the two diagonal configurations. This

is the contribution of only one excited configuration as schematically shown in Fig. 2a. There

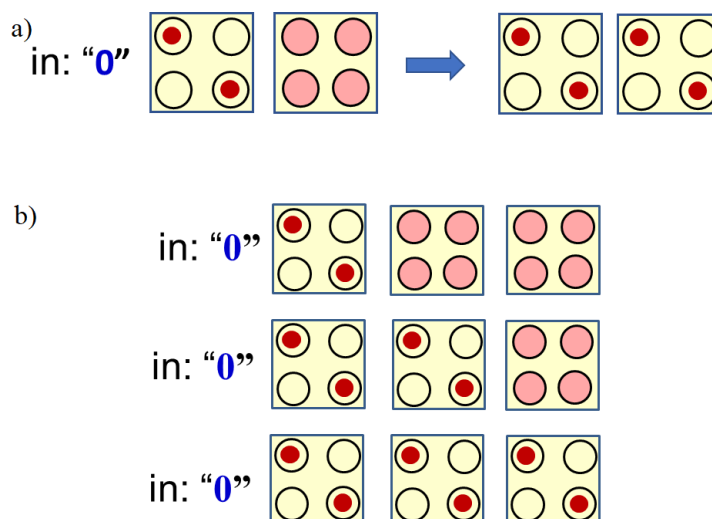


Figure 3. Illustration for the polarizing influence of the cell (input) on the neighboring cell (a) and current free transmission of information (b).

are four such contributions arising from four excited configurations, and so the absolute value of the second-order transfer matrix element connecting the two diagonal configurations proves to be equal to 4τ . As a result, the ground Coulomb manifold is split by the second-order transfer into two states representing the even and odd combinations of the diagonal configurations and separated by the energy gap 8τ as shown in 2b.

Up to now we have discussed the isolated (free) cells and considered only the intracell electronic interactions. When the cells are assembled in a QCA gate the constituent cells are subjected to the action of the electric field of the polarized neighboring cell (or cells), which removes the double degeneracy of the ground Coulomb manifold stabilizing one or another Boolean state. This is common for all QCA gates and lies in the background of the logical operations as schematically shown in Fig 3a. One can see that a preliminary polarized cell produces input **0** and its electric quadrupole field polarizes the neighboring cell creating the same state **0** (this corresponds to the minimum of Coulomb energy of a pair of interacting cells). The polarized cell transmits the information to the next cell and in this way the information propagates along the line of the cells as shown in Fig. 3b. This figure illustrates the function of QCA wire that transmits the binary information through the intercell Coulomb forces without flow of the electric current. Experimental demonstration of a binary wire for QCA has been reported in Ref. [37].

To characterize the intercell Coulomb interaction responsible for transmitting the binary information from cell to cell, let us consider a pair of interacting cells, where one of the cells termed “driver-cell” acts as a source of a quadrupole electric field and another cell (“working cell”) is subjected by the action of this field, which induces its polarization (Fig. 4). It is seen that in the limit of strong intracell Coulomb interaction when only the two d -configurations are involved one can use as a measure of the intercell interaction the energy gap $2u$ between the ground and the excited Coulomb manifolds of the pair of interacting cells, which is termed the “kink energy”. This energy is gained when the pair is aligned to have the same Boolean states.

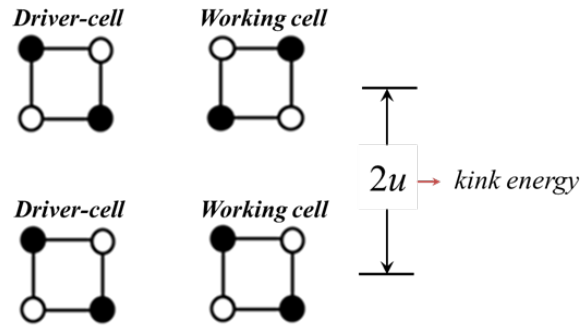


Figure 4. Schematic image of the intercell Coulomb interaction, which in the limit of strong intracell Coulomb interaction is associated with the kink energy.

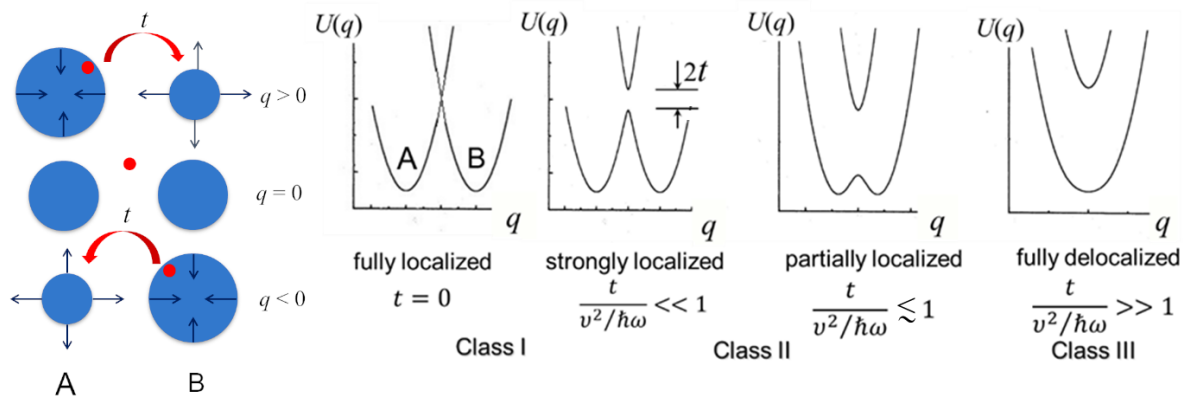


Figure 5. Illustration for the out-of-phase mode of a dimeric MV unit and its relevance to the electron transfer (left) and potential surfaces illustrating localization effect of the out-of-phase vibration in the dimeric MV unit and corresponding classification of MV (right).

3. Pseudo Jahn-Teller vibronic interaction in a molecular cell, localization vs delocalization

In the previous sections we have considered the interactions which acts in the molecule provided that positions of the ions are fixed in a certain frozen configurations that are independent of the state of the electronic pair. In addition to the electronic interactions so far discussed, the properties of MV molecules and, particularly, of molecular QCA cells are crucially dependent on the vibronic coupling that is the interaction of the excess electrons with the molecular vibrations. Being the polyatomic compounds, the MV molecules, and, particularly, the molecular QCA cells based on them have a large number of vibrational degrees of freedom, i. e. high-dimensional vibrational space. Fortunately, in many actual cases one can select only few active molecular vibrations, which are coupled to the highest extent to the motion of the excess electron(s) (see examples of detailed analysis in Refs. [38,39]). The vibrations, which produce the major effect on the electron localization in such systems are the “breathing” vibrations of the redox sites, e. g. the full-symmetric vibrations of the nearest ligand surroundings of the metal ions in MV clusters. The effect of these vibrations is quite similar to the polaronic effect in solids. Indeed, when the excess electron in MV unit enters the region of a redox center, it deforms the structure of the neighboring environment lowering the energy of the electron-vibrational system and producing thus a self-trapping effect. The depth of the potential well formed as a result of such self-trapping is a measure of the vibronic coupling. The “breathing” vibrations do not

change the distances between the redox sites and so they produce only local effect modulating the on-site energies of the excess electrons.

It is to be noted that the “breathing” vibrations confined to a definite small number of the atoms can be associated with the normal vibrations of the whole molecule only approximately.

Moreover, the definition of the redox site is not unconditional because the electronic density is spread out from the confined area of the metal center in metal complexes or from a definite set of the bonds in organic compounds in which the electronic density partially spreads out over the bridge connecting redox sites [38,39]. Nevertheless, a rather simple model so far described captures the most important features of mixed valency such as the existence of a potential barrier separating localized configurations and the related physical properties of MV molecules. The model based on the concept of the independent localized “breathing” modes is the conventional Piepho-Krausz-Schatz (PKS) vibronic model formulated for one-electron MV dimeric unit [40]. It is seen from Fig. 5 schematically showing the out-of-phase combination $(q_A - q_B)/\sqrt{2}$ of the coordinates of the “breathing” modes q_A and q_B that just this out-of-phase vibration is interconnected with the electron transfer between the redox centers A and B . The electronic energy spectrum of such dimer consists of the two levels of opposite parity separated by the gap $2t$. The interaction with the out-of-phase vibration mixes these levels, and hence we are dealing with the pseudo Jahn-Teller (JT) problem [41–43]. Figure 5 (right) shows the potential surfaces of the system $U(q)$ at different relative values of the transfer parameter t , the parameter of the vibronic coupling v and frequency of the PKS vibration ω . One can see that the PKS vibronic coupling produces effect of localization of the mobile electron. The extent of localization depends on the ratio t/E_{JT} , where $E_{JT} = v^2/2\hbar\omega$ is the vibronic stabilization energy, and varies from full localization (limit of weak transfer, Class I in the Robin & Day scheme) to full delocalization in the case of strong transfer or/and weak vibronic coupling.

In the case of square planar two-electron MV tetramer the effect of the vibronic interaction is quite similar. Thus, in the case of strong Coulomb interaction, the only active molecular vibration is involved, in course of which the two redox sites lying on one diagonal are expanded, while the remaining two sites lying on another diagonal are compressed as schematically shown in Fig. 6 in which the vibrational coordinate is denoted by q (we retain the same notation as for the dimeric system). Note that this vibration has the same frequency ω as the local breathing vibrations (the latter is assumed to be the same for sites with and without excess electron). As in a dimeric system, the main effect of such out-of-phase PKS vibration is the vibronic self-trapping effect. This effect can be intuitively understood from Fig. 6 showing the vibronic coupling effect not complicated by other interactions, particularly that uncontaminated by the effect of elastic interaction. Considering, for example, redox sites composed by positively charged transition metal ions and surrounding negatively charged ligands one can see that when the excess electron occupies a certain site this size is expanded minimizing the Coulomb repulsion between the excess electron and the negatively charged ligands. In contrast, when the site is empty the excess of positive charge appears on it, and so the site tends to be compressed. This produces stabilization of the states in which the two electrons are localized in one or another diagonal with respect to the state when the electronic pair is fully delocalized. The fully-delocalized state (state in which “half of electron” can be imagine on each site) corresponds to undistorted (reference) atomic configuration in which the sizes of all redox sites are equal, meanwhile the localized states are interrelated with the distorted vibrational configurations with $q < 0$ and $q > 0$ as shown in Fig. 6.

It is clear from the above discussion that the vibronic PKS coupling and the electron transfer

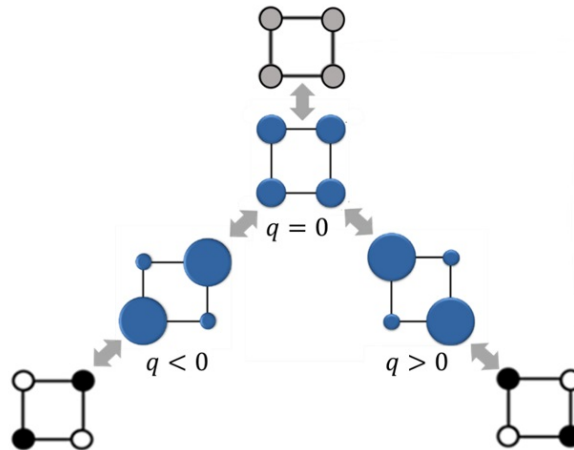


Figure 6. Illustration for the PKS vibronic coupling in the two-electron square-planar cell in the limit of strong intracell Coulomb repulsion. The active “out-of-phase” vibration with the coordinate q is shown. In course of this vibration the full-symmetric compression of the redox sites situated on one diagonal is accompanied by the full-symmetric expansion of the sites lying on another diagonal of the square. Due to the interaction of the excess electrons with this vibration the two diagonal charge configurations corresponding to the distorted vibrational configurations with $q < 0$ and $q > 0$ are stabilized with respect to the unpolarized ($\rho = 1/2$) charge configuration interrelated with the undistorted reference configuration ($q = 0$).

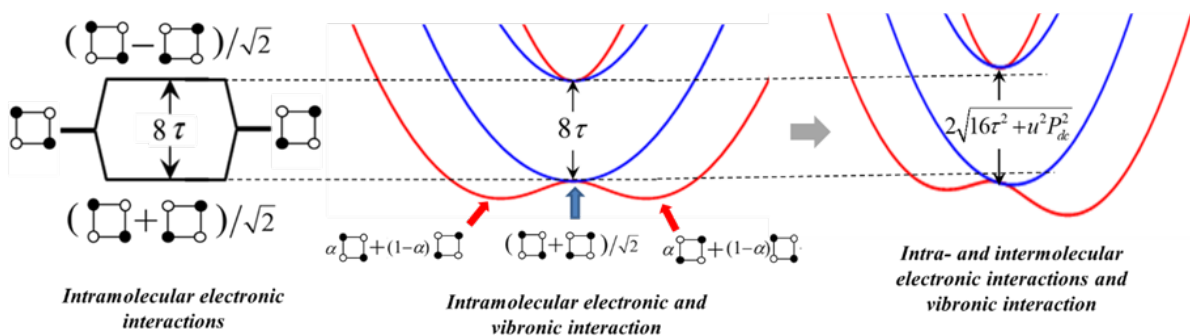


Figure 7. Effect of the effective second-order electron transfer (left), the combined effect of this transfer and the vibronic PKS coupling (middle), and the effect of both mentioned interactions and the intercell Coulomb interaction (right) for the case of strong intracell Coulomb interaction. Red lines - adiabatic potential curves for the case of strong pseudo-JT effect ($4\tau/(v/\hbar\omega) < 1$) stabilizing the two equivalent minima describing presumable localization of the electronic pair on one or another diagonal, blue lines – adiabatic potential curves for the case of weak pseudo-JT effect ($4\tau/(v/\hbar\omega) > 1$) when the excess electrons are fully delocalized in the only minimum.

(effective second-order transfer in the case of strong Coulomb interaction) produce competing effects on the ability of a MV molecule to localize electron at a definite site. While the PKS coupling tends to localize the electronic pair in a diagonal position, the electron transfer tends to delocalize it over two diagonals. The combined effect of these two interactions proves to be dependent on the relationship between the effective electron transfer matrix element 4τ and the vibronic stabilization energy $v^2/2\hbar\omega$. This is clear from Fig. 7 showing the adiabatic potential curves of the two-electron square cell in the case of strong Coulomb interaction. For a free cell these curves are shown in the middle part of Fig. 7. It is seen that in the undistorted (symmetric) reference configurations the energy pattern consists of the two levels separated by

the gap 8τ , i. e. it coincides with the pure-electronic energy pattern shown in the left part of Fig. 7. The out-of-phase PKS vibration mixes the two electronic states of opposite parity leading to the pseudo-Jahn-Teller effect. At $4\tau/(v/\hbar\omega) < 1$ the pseudo-JT effect is strong giving rise to the two minima in the lower branch of the adiabatic potential (red curves in Fig. 7). Each such minimum corresponds to the presumable localization of the electronic pair on one of the diagonals of the square as schematically shown in Fig. 7 through the populated sites of the tetramer.

The stronger is the vibronic coupling, the deeper are the minima, the higher is the barrier between them, and the higher is the extent of the localization in each minimum (the factor α is closer to 1, see middle part of Fig. 7). In contrast, when $4\tau/(v/\hbar\omega) > 1$ the lower branch of the adiabatic potential has the only minimum (blue curves in Fig. 7) corresponding to undistorted vibrational configuration and the electronic pair in this minimum is fully delocalized over two diagonals. In terms of the conventional Robin and Dey classification of MV compounds the systems with single well lower adiabatic potential curve belong to the fully-delocalized class **III**, while the systems characterized by the double-well curve belong to the class **II** or to the borderline between classes **II** and **III**. These features of the dimeric and tetrameric systems are qualitatively the same. Concluding this section, one should underly that the presence of the only PKS mode in the vibronic problem for the tetrameric system can be justified only in the case of strong Coulomb repulsion U , while in a more general case of arbitrary Coulomb repulsion we face a more complex vibronic problem of two levels-three vibrations (see full consideration of such multimode problem in Ref. [32]).

4. Cell-cell response function

The described picture of interacting cells (Figs. 3 and 4) ignores the tunneling of the excess charges between the redox sites or alternatively, second order electron transfer so far mentioned. Within frames of the model which accounts for the interelectronic Coulomb repulsion and electron transfer the degree of localization is determined by the competitive effects of the named interactions and also by the strength of the external field. In fact, the full localization of the electronic pair on one (AC) or another (BD) diagonal can appear only provided that the quadrupole field acting on the cell is strong enough to be able to overcome the tunneling.

Now let us introduce some functional characteristics related to a simple qualitative picture so far considered. The QCA devices represent arrays of cells interacting with each other through the Coulomb forces (for example, a wire in Fig. 3b). In this case the field acting on a definite working cell (wc) is created by the previously polarized neighboring driver-cell (dc). The polarized driver-cell can be regarded as an electric quadrupole (left part of Fig. 8a) in which the electronic populations (electronic densities) of the sites located at a certain diagonal are equal to ρ_{dc} , while the populations of the sites belonging to another diagonal are $1 - \rho_{dc}$. Consequently, the charges located at the sites are $e\rho_{dc}$ and $e(1 - \rho_{dc})$, where e is the electron charge. The full polarization of the driver-cell ($\rho_{dc} = 0$ and 1) corresponds to the Boolean states **0** and **1**. The quadrupole electric field created by the polarized driver-cell acts on the working cell (right part of Fig. 8a) inducing its polarization or, in other words, inducing a quadrupole electric moment on the working cell.

As distinguished from quantum computers, the QCA computing devices are usually referred to as classical ones in the sense that their performance is based on the classical Coulomb forces governing the information flow. At the same time the phenomenon of partial localization crucially affecting the characteristics of the QCA cells (see next section) is essentially quantum effect

arising from the mixing of the wave-functions belonging d - and n -configurations. Moreover, the tunneling between localized configuration is an essentially quantum effect. In this context the conventional terminology referring the QCA devices as classical has a conditional meaning.

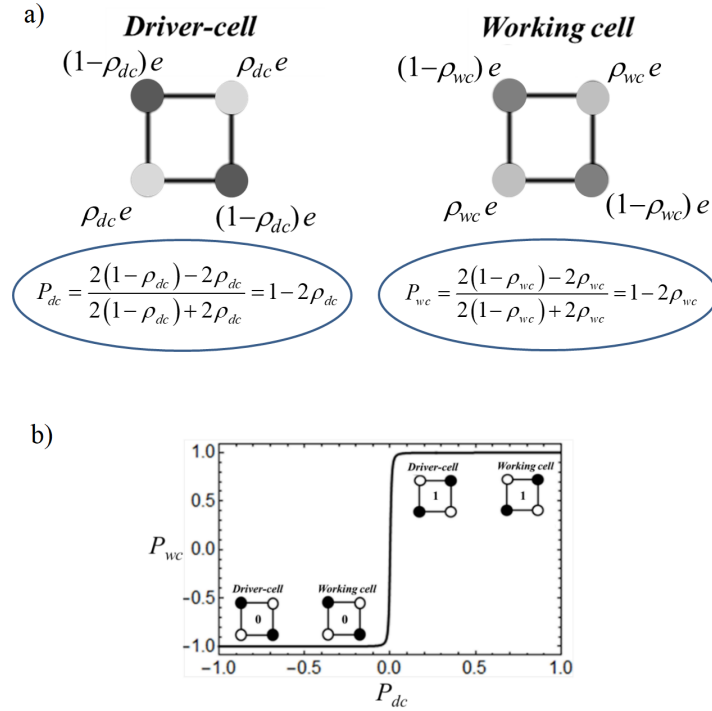


Figure 8. (a) Pair of the two-electron tetrameric square-planar QCA cells representing electric quadrupoles. Driver-cell (left part) with polarization P_{dc} acts as a source of the quadrupole field, which induces polarization P_{wc} on the working cell (right). Polarization is defined as a normalized difference between the electronic populations of the sites in one diagonal and those in another diagonal; (b) illustration for the cell-cell response function $P_{wc}(P_{dc})$.

The quadrupole electric field created by the polarized driver-cell acts on the working cell (right part of Fig. 8a) inducing its polarization or, in other words, inducing the quadrupole electric moment on the working cell. As a measure of polarization of the cell we use the normalized excess of the electronic density of one diagonal over the density of another diagonal as explicitly defined in Fig. 8a, and just call this value “polarization” [44]. It is assumed that the polarization of the driver-cell P_{dc} is created before the logical operation in the QCA gate begins and then (in course of the computational pipeline) can be changed in a controlled manner from $P_{dc} = -1$ (Boolean state **1**) to $P_{dc} = 1$ (state **0**). In course of repolarization the driver cell passes through the unpolarized state $P_{dc} = 0$ in which all sites are populated by the “half of electron” ($\rho_{dc} = 1/2$). The dependence of the induced polarization P_{wc} in the working cell on the inducing polarization P_{dc} of the driver cell is called “cell-cell response function”, i. e. $P_{wc} = f(P_{dc})$ or $P_{wc}(P_{dc})$.

The character of this dependence shows the efficiency with which repolarization of the driver-cell can force switching of the working cell between the two Boolean states. Alternatively, an effectiveness of the working cell repolarization under the action of the field of the driver-cell characterizes the efficiency of the information flow and, ultimately, the performance of the device. In ideal, this dependence should have strongly non-linear (stepwise) shape as schematically shown in Fig. 8b along with the schemes of the initial and final states of the driver and working cells. Such shape of the cell-cell response function means that even a very weak quadrupole field

of the driver-cell is able to fully polarize the working cell, and this is just what is required to ensure efficiency of propagation of the binary information from cell to cell within a QCA gate. The strong non-linear cell-cell response is the first key requirement the MV molecule should meet to be suitable as QCA cells. The second requirement, that of low power dissipation, will be discussed later on.

It is worth to make a note regarding an important role of the non-linearity of the cell-cell response. In real systems the imperfections such as random variations in the size of the cells, errors in the intercellular spacing, random fields, etc. always present. It has been demonstrated that the highly nonlinear cell-cell response acts to correct mistakes and restore the signal level [37].

5. Effects of different interactions on the cell-cell response

The difference in the extent of the electron delocalization over two diagonal positions plays a pivotal role in the properties of QCA cell. Indeed, the presumable localization of the electronic pair along one diagonal in the adiabatic potential minimum means that the cell residing in this minimum is already partially polarized. Of course, in the absence of the external electric field such polarization can only exist in the sense of broken symmetry, because there are two equivalent minima with polarizations having opposite signs and so in the stationary (in the quantum-mechanical sense) states resulting from the tunneling processes the overall polarization is zero. Nevertheless, such broken-symmetry polarization is removed, i. e. transformed into a definite (“genuine”) polarization of the cell when the external quadrupole field having lower symmetry is applied. Indeed, such field stabilizes one of the minima (right part of Fig. 7) with polarization already prepared by the vibronic coupling but the last is enhanced by the field. In contrast, if a free cell is characterized by the adiabatic potential curve having single delocalized minimum (unpolarized state) the system is insensitive to the field, or alternatively, much stronger field is required to polarize such cell.

All of the above observations create a belief that weakly delocalized tetramers characterized by the vibronic coupling dominating over the effective electron transfer should exhibit a strong non-linear cell-cell response, which is one of the key requirements the MV molecule should satisfy to have chance to be used as QCA cell. In many cases, especially for moderate pseudo-JT vibronic coupling, the evaluation of the cell-cell response function should be based on the quantum-mechanical solution of the vibronic problem (see details of such calculations in ref. [28]). Indeed, in the case of a moderate vibronic coupling the adiabatic approximation fails, and so the solution of the quantum-mechanical (dynamic) vibronic pseudo-JT problem is required.

Figures 9a and 9c demonstrate the effects of different involved intracell interactions on the cell-cell response function. Thus, it is seen from Fig. 9a that the systems characterized by smaller values of τ exhibit stronger non-linearity of the cell-cell response functions, other things being equal. Also, as follows from Fig. 9c, the cell-cell response is stronger and exhibits higher non-linearity for systems with stronger vibronic coupling. Finally, Fig. 9e shows the dependence of the cell-cell response on the strength of the intercell interaction. It is not unexpected result that the cell-cell response proves to be stronger for larger kink energies.

6. Power dissipation in a tetrameric molecular cell evaluated within the vibronic approach

The urgency of the problem of heat dissipation is dictated by the fact that high heat release is one of the main obstacles to the further miniaturization of electronic devices. Considering the vibronic approach to the study of molecular cell in context of the functional properties

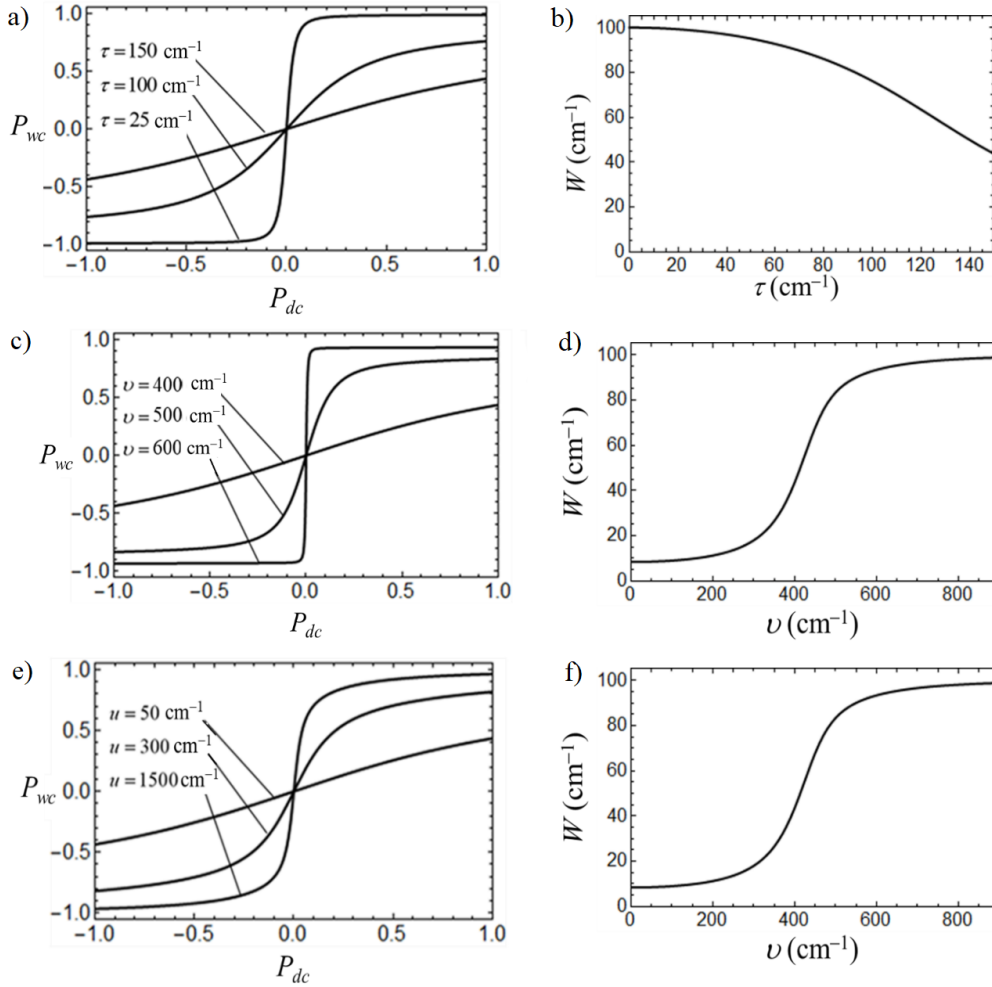


Figure 9. Cell-cell response functions (a, c, e) and heat release values (b, d, f) evaluated at $\hbar\omega = 200 \text{ cm}^{-1}$, $\nu = 400 \text{ cm}^{-1}$, $u = 200 \text{ cm}^{-1}$ (a, b), $\hbar\omega = 200 \text{ cm}^{-1}$, $\tau = 150 \text{ cm}^{-1}$, $u = 50 \text{ cm}^{-1}$ (c, d), and $\hbar\omega = 200 \text{ cm}^{-1}$, $\nu = 400 \text{ cm}^{-1}$, $\tau = 200 \text{ cm}^{-1}$ (e, f). The cell-cell response functions are evaluated at three values of the remaining parameter as shown in the plots a, c and e. The heat release values are calculated as functions of the remaining parameters (b, d, f).

of QCA cells one should focus on the heat release that necessarily accompanies the structural transformations of a cell in course of its action. This is an emerging problem [45–48] in view of the potential advantages of molecular QCA based on the currentless way of the information flow, which is expected to ensure a low heat release. In general, evaluation of power dissipation rises the problem of accurate accounting for the interaction of the electronic subsystem and molecular vibrations with the thermal bath (phonons) and subsequent solution of Lindblad or Redfield master equation [48] for the reduced density matrix. Nevertheless, in a particular but important situation the evaluation of the heat release can be essentially simplified [34]. This is the case of fast nonadiabatic switching of the electric field acting on the working cell from the side of the driver-cell, for which the heat release is known to be maximal.

Leaving the details of such calculations outside the scope of this brief review article (see refs. [34] for the details), let us focus on the main results. Figures 9b, 9d and 9f show sample calculations illustrating the influence of different interactions on the specific heat release W that means heat release per one cell occurring in course of one switching cycle. It is seen from Fig. 9b that heat release is lower for cells characterized by larger effective transfer parameter τ . Also,

the heat release is lower in the case of weaker vibronic coupling (Fig. 9d). Finally, the weaker is the interaction between the cells, the lower is the power dissipation, with the dependence of the heat release on the kink energy being practically linear (Fig. 9f).

7. Some theoretical hints for the cell design

It would seem, as follows from Fig. 9b and 9d, that to reduce heat release it is necessary to use highly delocalized MV tetramers. This, is however, in conflict with the requirement of strong non-linear cell-cell response for which one needs molecules having rather weak delocalization. There is, however, a way to reconcile these contradictory tendencies. To mark this way, let us notice that the heat release saturates with the increase of vibronic coupling or with the decrease of the effective electron transfer reaching the maximal value that is just the kink energy (see Figs. 9b and 9d). This means that even provided weak delocalization the heat release proves to be low provided that the cell-cell interaction is weak or alternatively, the kink energy is small. At the same time for such low extent of the electron delocalization even very weak quadrupole field corresponding to small kink energy is able to ensure strong non-linear cell-cell response. This means that weakly interacting (e. g. far apart disposed) cells exhibiting weak electron delocalization are expected to simultaneously provide both strong non-linear cell-cell response and low power dissipation. Therefore, one arrives to an important conclusion that such cells meet both considered key requirements for the MV molecules which could act as QCA cells. The established hint for design seems to be a useful guide in the search of new MV compounds which could be promising for QCA implementations.

8. Concluding remarks

In this short review article, we have presented at a simple descriptive level the main principles of molecular QCA and a simplified model of the tetrameric MV molecules plying a role of the cell in molecular QCA. The model includes Coulomb repulsion between two electrons in the cell and their interaction with the electric field of the neighboring cell that plays the role of the driver-cell. The vibronic pseudo-JT interaction is also an important ingredient of the model. The physical role of these interactions is revealed and the conditions are formulated under which a MV molecule could be potentially applicable as a cell in the QCA devices. The physical features behind these conditions are the ability of the MV molecules to be efficiently switched between two logical states which assumes high polarizability manifesting itself in a strong non-linear cell-cell response and a low heat release caused by molecular rearrangements accompanying logical operations. Finally, the optimal parametric regime ensuring simultaneous fulfillment of the competing requirements so far mentioned is discussed.

Acknowledgments

The work was in part (evaluation of heat release in course of nonadiabatic switching) performed with financial support from the Russian Science Foundation (V. B., A. P., project no. 20-13-00374-II) and in part (evaluation and analysis of cell-cell response functions) with financial support from the Ministry of Science and Higher Education of the RF (V. B., A. P., state assignment No. 124013100858-3).

References

1. Lent C. S., Tougaw P., Porod W., Bernstein G. H., *Nanotech.* **4**, 49 (1993).
2. Lent C. S., Tougaw P. D., Porod W., *Appl. Phys. Lett.* **62**, 714 (1993).

3. Lent C. S., Tougaw P. D., *J. Appl. Phys.* **74**, 6227 (1993).
4. Lent C. S., Isaksen B., Lieberman M., *J. American Chem. Soc.* **125**, 1056 (2003).
5. Tougaw P. D., Lent C. S., *J. Appl. Phys.* **75**, 1818 (1994).
6. Lent C. S., Tougaw P. D., *Proc. IEEE* **85**, 541 (1997).
7. Porod W., Lent C., Bernstein G. H., Orlov A. O., Hamrani I., Snider G. L., Merz J. L., *Inter. J. Electron.* **86**, 549 (1999).
8. Tóth G., Lent C. S., *J. Appl. Phys.* **85**, 2977 (1999).
9. Lent C. S., *Science* **288**, 1597 (2000).
10. Tóth G., Lent C. S., *Phys. Rev. A* **63**, 052315 (2001).
11. Qi H., Sharma S., Li Z., Snider G. L., Orlov A. O., Lent C. S., Fehlner T. P., *J. Amer. Chem. Soc.* **125**, 15250 (2003).
12. Qi H., Gupta A., Noll B. C., Snider G. L., Lu Y., Lent C., Fehlner T. P., *J. Amer. Chem. Soc.* **127**, 15218 (2005).
13. Lu Y., Lent C. S., *J. Comp. Electron.* **4**, 115 (2005).
14. Lu Y., Quardokus R., Lent C. S., Justaud F., Lapinte C., Kandel S. A., *J. Amer. Chem. Soc.* **132**, 13519 (2010).
15. Braun-Sand S. B., Wiest O., *J. Phys. Chem. A* **107**, 285 (2003).
16. Zhao Y., Guo D., Liu Y., He C., Duan C., *Chem. Comm.* , 5725 (2008).
17. Schneider B., Demeshko S., Neudeck S., Dechert S., Meyer F., *Inorg. Chem.* **52**, 13230 (2013).
18. Lau V. C., Berben L. A., Long J. R., *J. Amer. Chem. Soc.* **124**, 9042 (2002).
19. Palii A., Aldoshin S., Zilberg S., Tsukerblat B., *Phys. Chem. Chem. Phys.* **22**, 25982 (2020).
20. Palii A., Zilberg S., Rybakov A., Tsukerblat B., *J. Phys. Chem. C* **123**, 22614 (2019).
21. Ruben M., Rojo J., Romero-Salguero F. J., Uppadine L. H., Lehn J.-M., *Angewandte Chem. Internat. Edit.* **43**, 3644 (2004).
22. Tsukerblat B., Palii A., Clemente-Juan J. M., *Pure Appl. Chem.* **87**, 271 (2015).
23. Tsukerblat B., Palii A., Clemente-Juan J. M., Coronado E., *J. Chem. Phys.* **143** (2015).
24. Palii A., Tsukerblat B., Clemente-Juan J. M., Coronado E., *J. Phys. Chem. C* **120**, 16994 (2016).
25. Tsukerblat B. S., Palii A., Clemente-Juan J., Suaud N., Coronado E., *Acta Phys. Polon. A* **133**, 329 (2018).
26. Tsukerblat B., Palii A., Aldoshin S., *Israel J. Chem.* **60**, 527 (2020).

27. Tsukerblat B., Palii A., Aldoshin S., *Magnetochem.* **7**, 66 (2021).
28. Palii A., Aldoshin S., Tsukerblat B., *Dalton Transact.* **51**, 286 (2022).
29. Palii A., Rybakov A., Aldoshin S., Tsukerblat B., *Phys. Chem. Chem. Phys.* **21**, 16751 (2019).
30. Clemente-Juan J. M., Palii A., Coronado E., Tsukerblat B., *J. Chem. Theor. Comput.* **12**, 3545 (2016).
31. Tsukerblat B., Palii A., Zilberg S., Korchagin D., Aldoshin S., Clemente-Juan J. M., *J. Chem. Phys.* **157** (2022).
32. Palii A., Belonovich V., Aldoshin S., Tsukerblat B., *Chem. Phys.* **563**, 111679 (2022).
33. Palii A., Aldoshin S., Tsukerblat B., *Magnetochem.* **8**, 92 (2022).
34. Palii A., Belonovich V., Tsukerblat B., *Phys. Chem. Chem. Phys.* **25**, 17526 (2023).
35. Palii A., Belonovich V., Aldoshin S., Zilberg S., Tsukerblat B., *J. Phys. Chem. A* **127**, 9030 (2023).
36. Macrae R. M., *J. Phys. Chem. Solids* **177**, 111303 (2023).
37. Orlov A. O., Amlani I., Toth G., Lent C. S., Bernstein G. H., Snider G. L., *Appl. Phys. Lett.* **74**, 2875 (1999).
38. Zilberg S., Stekolshik Y., Palii A., Tsukerblat B., *J. Phys. Chem. A* **126**, 2855 (2022).
39. Zilberg S., Tsukerblat B., Palii A., *J. Phys. Chem. A* **127**, 3281 (2023).
40. Piepho S. B., Krausz E. R., Schatz P., *J. Amer. Chem. Soc.* **100**, 2996 (1978).
41. Englman R., *The Jahn-Teller effect in molecules and crystals* (Wiley-Interscience, New York, 1972) 350 p.
42. Bersuker I. B., Polinger V. Z., *Vibronic interactions in molecules and crystals*, Vol. 49 (Springer-Verlag, Berlin, 1989) 422 p.
43. Tsukerblat B., Klokishner S., Palii A., “Jahn–Teller Effect in Molecular Magnetism: An Overview,” in *The Jahn-Teller Effect: Fundamentals and Implications for Physics and Chemistry*, edited by Köppel H., Yarkony D. R., Barentzen H. (Springer Berlin Heidelberg, 2009) pp. 555–619.
44. Tougaw P. D., Lent C. S., Porod W., *J. Appl. Phys.* **74**, 3558 (1993).
45. Timler J., Lent C. S., *J. Appl. Phys.* **91**, 823 (2002).
46. Rahimi E., *Micro & Nano Lett.* **11**, 369 (2016).
47. Rahimi E., Reimers J. R., *Phys. Chem. Chem. Phys.* **20**, 17881 (2018).
48. Pidaparthi S. S., Lent C. S., *J. Appl. Phys.* **131** (2022).